Neurocomputing 248 (2017) 19–27

Contents lists available at ScienceDirect

Neurocomputing

journal homepage: www.elsevier.com/locate/neucom

# Stabilization of desired periodic orbits in dynamic binary neural networks

Ryuji Sato, Toshimichi Saito*

*Department of Electrical and Electronic Engineering, Faculty of Science and Engineering, Hosei University, Koganei-shi, Tokyo 184–8584, Japan*

ARTICLE INFO

*Article history:*
Received 30 June 2016
Revised 1 October 2016
Accepted 23 October 2016
Available online 7 March 2017

*Keywords:*
Dynamic binary neural network
Periodic orbit
Stability
Stabilization

ABSTRACT

A dynamic binary neural network is a simple two-layer network with a delayed feedback and is able to generate various binary periodic orbits. The network is characterized by the signum activation function, ternary connection parameters, and integer threshold parameters. The ternary connection brings benefits to network hardware and to computation costs in numerical analysis. In order to stabilize a desired binary periodic orbit, a simple evolutionary algorithm is presented. The algorithm uses individuals corresponding to the ternary connection parameters and one zero element is inserted into each individual. Each individual is evaluated by two feature quantities that characterize the stability of the periodic orbit. The zero-insertion is able to reinforce the stability and is convenient to reduce power consumption in a hardware. Applying the algorithm to a class of periodic orbits, the stabilization capability is investigated. Some of the periodic orbits are applicable to control signals of switching power converters.



## 1. Introduction

Applying a delayed feedback to the two-layer neural network, the dynamic binary neural network (DBNN) is constructed [1,2,3]. The DBNN is characterized by the signum activation function [4–7], ternary connection parameters and integer threshold parameters. Comparing an input with the threshold, the signum activation function outputs a binary value. The ternary connection is convenient in a hardware implementation by digital circuits as suggested in [8]. Depending on the parameters and initial condition, the DBNN can generate various binary periodic orbits (BPOs). The dynamics of the DBNN is integrated into the digital return map (Dmap) on a set of points [3]. The Dmap can be regarded as a digital version of an analog return map such as the logistic map [9]. The Dmap is useful in visualization/consideration of the dynamics. Since the state variables are binary and connection parameters are ternary, the dynamics of the Dmap/DBNN can be calculated by the integer arithmetic and the computation costs can be reduced in numerical analysis [3].

The DBNN is a kind of digital dynamical systems where time, state, and parameters are all discrete [10–15]. The digital dynamical systems have been applied to engineering systems. For example, the cellular automata can generate various spatio-temporal patterns and have been applied to signal processing [10–12]. The digital spiking neurons can generate various spike-trains and have been applied to ultra-wide-band communications [13,14]. The BPOs of the DBNN have been applied to control signals of switching power converters [3]. That is, study of such systems is significant in both fundamental and application viewpoints.

This paper studies stability and stabilization of a desired BPO of the DBNNs.

It goes without saying that the stability is an important concept in analysis of nonlinear phenomena and corresponds to robust/reliable system operation in engineering applications. Although there exist several methods to store periodic orbits into neural networks [15–18], stabilization of the stored periodic orbits has not been considered sufficiently.

First, using the Dmap, we define two kinds of stabilities of a BPO: global stability such that all the initial points fall eventually into the BPO and uniform stability such that all the initial points fall uniformly into the BPO. The uniform stability is a special case of the global stability. In analog dynamical systems, definition of stability has been studied sufficiently [9]. However, the definition cannot be applied to digital dynamical systems. Because the "analog" stability is based on mapping from a set of real numbers whereas the "digital" stability is based on mapping from a set of binary numbers. Hence we have defined the stabilities of the BPO.

Second, we present two feature quantities $\alpha$ and $\beta$ that characterize the global and uniform stabilities, respectively. The feature quantities are used to evaluate the stabilities of a desired BPO. The evaluation is indispensable in the stabilization, however, feature

* Corresponding author.
*E-mail address:* tsaito@hosei.ac.jp (T. Saito).

http://dx.doi.org/10.1016/j.neucom.2016.10.084
0925-2312/

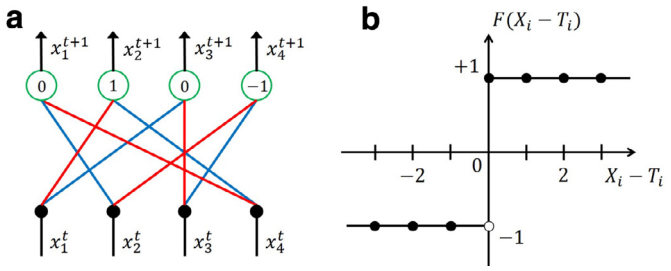


**Fig. 1.** DBNN. (a) Network. Red (light gray) and blue (gray) segments represent $w_{ij} = +1$ and $w_{ij} = -1$, respectively. $w_{ij} = 0$ means no connection. The threshold parameters $T_i$ are shown in the green circles. (b) Signum activation function.

quantities for the evaluation have not been presented in previous works.

Third, we present a simple evolutionary algorithm (SES) for uniform stabilization of a desired BPO. The SES uses individuals corresponding to a set of ternary connection parameters and one zero element is inserted into each individual. The zero-insertion corresponds to wire cutting in a hardware that is convenient to reduce power consumption. For the storage of a BPO, we have a simple method based on the correlation learning (CL-based learning, [1,18]). If the CL-based learning can store a desired BPO into the DBNN, the set of connection parameters is used as an initial individual. The quantity $\beta$ is used to evaluate each individual in the evolution process. In order to help the evaluation by $\beta$, the quantity $\alpha$ is also used. The SES is simpler and the computation costs are lower than the existing methods based on the genetic algorithm (GA) [1,2]. The GA-based methods use stochastic operators such as the elite strategy and mutation, whereas the SES does not use such stochastic operators.

In order to investigate the stabilization capability of the SES, we have performed numerical experiments for a basic class of BPOs. The BPOs can be stored into the DBNN and some of them are applicable to control signals of switching circuits [19–21]. Applying the SES to the BPOs, we have confirmed that the individuals can evolve and the zero-insertion is effective to reinforce the uniform stability of BPOs.

It should be noted that this is the first paper of the definition of the uniform stability, of the feature quantity to evaluate the uniform stability, and of the uniform stabilization.[1]

The rest of this paper is organized as follows. In Sections 2 and 3, we introduce the DBNN, the Dmap, and the CL-based learning. In Section 4, we define the stabilities and present the SES. Sections 5 and 6 show several numerical results to evaluate the SES. Section 7 concludes the paper.

## 2. Dynamic binary neural networks and periodic orbits

Applying a delayed feedback to the two-layer network, the dynamic binary neural network (DBNN) is constructed as shown in Fig. 1(a) [1,2,3]. The dynamics is described by

$$x_i^{t+1} = F\left(\sum_{j=1}^{N} w_{ij} x_j^t - T_i\right), \quad i = 1 \sim N$$

$$F(X_i - T_i) = \begin{cases} +1 & \text{if } X_i \geq T_i \\ -1 & \text{if } X_i < T_i \end{cases}, \quad X_i \equiv \sum_{j=1}^{N} w_{ij} x_j^t \tag{1}$$

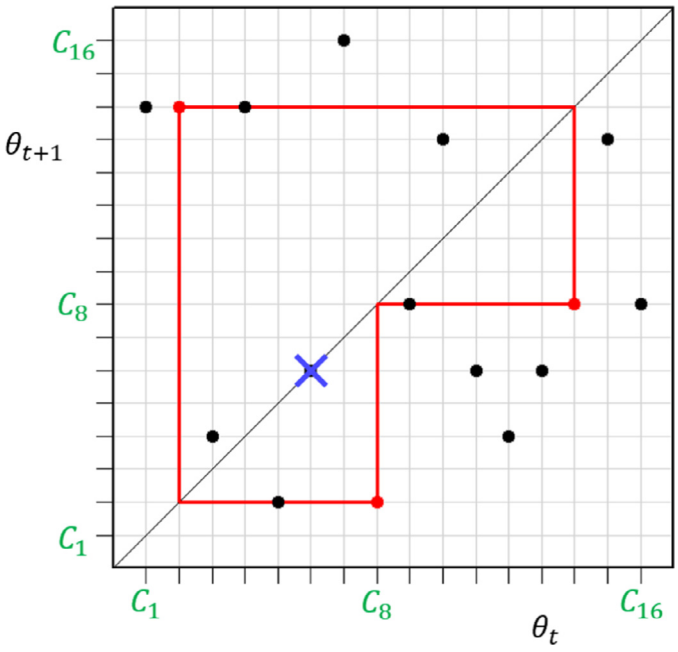


**Fig. 2.** A Dmap of the DBNN. The red (light gray) orbit is a BPO with period 3. The cross is a fixed point.

where $\boldsymbol{x}^t \equiv (x_1^t, \ldots, x_N^t)$ is a binary state vector at discrete time $t$ and $x_i^t \in \{-1, +1\} \equiv \boldsymbol{B}$ is the $i$th element. Comparing $X_i$ with a threshold $T_i$, the signum activation function $F$ outputs +1 or −1. The signum activation function is used in various artificial neural networks including the binary neural networks (BNNs [4–7]).

We abbreviate Eq. (1) by $\boldsymbol{x}^{t+1} = \boldsymbol{F}_D(\boldsymbol{x}^t)$. As an initial state vector $\boldsymbol{x}^1$ is applied, the DBNN generates a sequence of binary vectors $\{\boldsymbol{x}^t\}$. The connection parameters $w_{ij}$ are ternary and the threshold parameters $T_i$ are integer:

$$w_{ij} \in \{-1, 0, +1\}, \quad T_i \in \{0, \pm 1, \pm 2, \pm 3, \ldots\} \tag{2}$$

Since $X_i - T_i$ is an integer as shown in Fig. 1(b), the dynamics of the DBNN can be calculated by the integer arithmetic and the computation costs can be reduced in numerical analysis.[2] As stated earlier, the ternary connection parameters are convenient in a hardware implementation by digital circuits as suggested in [8]. Since $w_{ij} = 0$ corresponds to wire cutting in a hardware, the zero elements can reduce power consumption.

In order to visualize the DBNN dynamics, we introduce the Dmap. The domain of the DBNN is a set of binary vectors $\boldsymbol{B}^N$ and the set is equivalent to a set of $2^N$ points:

$$L_N \equiv \{c_1, \ldots, c_{2^N}\}, \quad c_i = \frac{i}{2^N} \equiv h(b_i), \quad b_i \in \boldsymbol{B}^N \tag{3}$$

where $i$ denote decimal integers of $b_i$ in the binary coding. The fractions $1/2^N$ to $2^N/2^N$ correspond to the $2^N$ elements of $\boldsymbol{B}^N$. Using Eq. (3), the dynamics of the DBNN can be integrated into the Dmap on $L_N$.

$$\theta^{t+1} = f(\theta^t), \quad \theta^t \in L_N, \quad f(\theta) \equiv h \circ \boldsymbol{F}_D \circ h^{-1}(\theta) \tag{4}$$

Fig. 2 illustrates a Dmap for $N = 4$ where the binary code is used to express $L_4 = \{c_1, \ldots, c_{24}\}$: $c_1 \equiv (-1, -1, -1, -1)$, $c_2 \equiv (-1, -1, -1, +1)$, $\ldots$, $c_{24} \equiv (+1, +1, +1, +1)$. Since the number of points is $2^N$, direct memory of all the inputs/outputs becomes hard as $N$ increases. However, in the DBNN, the number of parameters

[1] An extended version of our conference paper [3] where definition of stability and numerical analysis of stabilization are insufficient.

[2] Networks with real connection parameters have been considered in the statistical neuro-dynamics theory [22].

is $N^2+N$. The Dmap is useful in visualization and analysis of the DBNN. Since the number of the points is finite, the steady state of the Dmap must be a periodic orbit defined as the following.

**Definition 1.** A point $\theta_p \in L_D$ is said to be a periodic point (PEP) with period $p$ if $f^p(\theta_p)=\theta_p$ and $f(\theta_p)$ to $f^p(\theta_p)$ are all different where $f^k$ is the $k$-fold composition of $f$. Especially, a PEP with period 1 is referred to as a fixed point. A sequence of the PEPs, $\{F(\theta_p),\ldots,F^p(\theta_p)\}$, is said to be a periodic orbit (PEO). A PEO of the Dmap is equivalent to a BPO of the DBNN.

In Fig. 2, the Dmap has a PEO with period 3 that corresponds to a BPO with period 3 of the DBNN:

$$c_2 \equiv (-1,-1,-1,+1) \to c_{14} \equiv (+1,+1,-1,+1) \to c_8 \equiv (-1,+1,+1,+1) \to c_2 \to \cdots \tag{5}$$

## 3. Storage of a desired BPO

We consider storage of one BPO with period $p$:

$$\boldsymbol{z}^1,\boldsymbol{z}^2,\ldots,\boldsymbol{z}^p,\boldsymbol{z}^{p+1},\ldots \tag{6}$$

$$\begin{cases}\boldsymbol{z}^i=\boldsymbol{z}^j & \text{for } |i-j|=np\\ \boldsymbol{z}^i\neq\boldsymbol{z}^j & \text{for } |i-j|\neq np\end{cases} \tag{6}$$

where $n$ denotes positive integers. This BPO is referred to as a teacher signal binary periodic orbit (TBPO) and will be an object of stabilization. In the Dmap, this TBPO corresponds to one teacher signal periodic orbit (TPEO) with period $p$ consisting of teacher signal periodic points (TPEPs) in the Dmap. For convenience, we decompose the TBPO in Eq. (6) into $p$ pieces of teacher signal pairs:

$$(\boldsymbol{\xi}^\tau,\boldsymbol{\eta}^\tau)=(\boldsymbol{z}^\tau,\boldsymbol{z}^{\tau+1}),\quad \tau\in\{1,\ldots,p\} \tag{7}$$

where $\boldsymbol{\eta}^p=\boldsymbol{z}^{p+1}=\boldsymbol{z}^1$. $\xi^\tau$ and $\eta^\tau$ correspond to TPEPs in the Dmap. The TBPO is stored into the DBNN if parameters ($w_{ij}$ and $T_i$) can realize

$$\boldsymbol{\eta}^\tau=\boldsymbol{F}_D(\boldsymbol{\xi}^\tau),\quad \tau\in\{1,\ldots,p\} \tag{8}$$

Eq. (8) is guaranteed if the following is satisfied

$$\sum_{j=1}^{N} w_{ij}\xi_j^\tau \equiv r(i,\tau)\geq T_i \quad \text{for } i \text{ such that } \eta_i^\tau=+1$$

$$\sum_{j=1}^{N} w_{ij}\xi_j^\tau \equiv l(i,\tau)< T_i \quad \text{for } i \text{ such that } \eta_i^\tau=-1 \tag{9}$$

Hence we obtain a sufficient condition for the storage:

$$L(i)<R(i) \quad \text{for all } i$$
$$L(i)=\max_\tau l(i,\tau),\quad R(i)=\min_\tau r(i,\tau) \tag{10}$$

Note that this condition is determined by a desired TBPO and connection parameters. If we can obtain connection parameters that satisfy Eq. (10) then we give the threshold parameters as the following.

$$T_i=\begin{cases}(L(i)+R(i))/2 & \text{if } (R(i)-L(i))=\text{even}\\ (L(i)+R(i)+1)/2 & \text{if } (R(i)-L(i))=\text{odd}\end{cases} \tag{11}$$

If the $i$th element of the TBPO is fixed to $+1$ (respectively, $-1$) then $L(i)$ (respectively, $R(i)$) does not exist. In such a case, $T_i$ is given by

$$T_i=\begin{cases}R(i)-1 & \text{if } \eta_i^\tau=+1 \text{ for } 1\leq\tau\leq p\\ L(i)+1 & \text{if } \eta_i^\tau=-1 \text{ for } 1\leq\tau\leq p\end{cases} \tag{12}$$

These threshold parameters guarantee storage of the TBPO.

As a simple method to store a TBPO, we have presented the CL-based learning [1,2,3] such that the connection parameters are given by ternarizing the results of the correlation learning:

$$w_{ij}=\begin{cases}+1 & \text{for } c_{ij}>0\\ 0 & \text{for } c_{ij}=0\\ -1 & \text{for } c_{ij}<0\end{cases},\quad c_{ij}=\sum_{\tau=1}^{p}\eta_i^\tau\xi_j^\tau \tag{13}$$

If these connection parameters satisfy Eq. (10) then the threshold parameters are given by Eqs. (11) or (12). The obtained parameters guarantee storage of the TBPO.

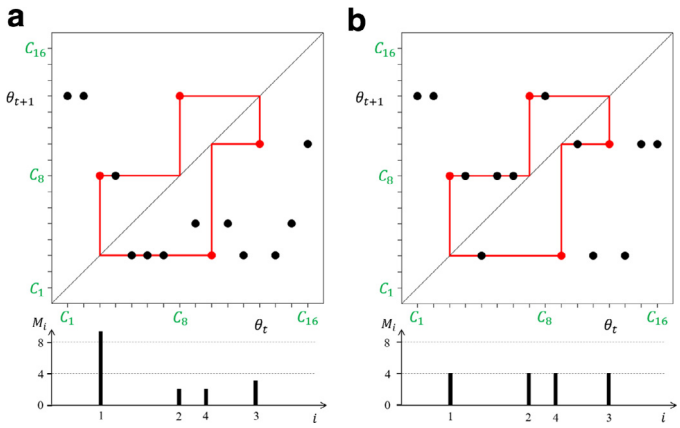


**Fig. 3.** Stability of a TPEO. (a) Globally stable TPEO in the Dmap and its histogram of the number of initial points falling into the TPEPs. ($\alpha=16/16$, $\beta=2/4$) (b) Uniformly stable TPEO ($\alpha=16/16$, $\beta=4/4$).

## 4. Stabilization of a desired BPO

In this main section, we define stabilities of the TPEO and present the simple evolutionary stabilization algorithm (SES). Since a PEO (consisting of PEPs) of the Dmap is equivalent to a BPO of the DBNN, we use the term PEO (and PEP) instead of the term BPO in the context. First, we give a basic definition of transient phenomena.

**Definition 2.** A point $\theta_e \in L_D$ is said to be an eventually periodic point (EPP) if $\theta_e$ is not a PEP but falls into some PEP $\theta_p$: $F^q(\theta_e)=\theta_p$ where $q$ is some positive integer. An orbit started from an EPP falls into either PEP.

In Fig. 3, black points correspond to EPPs falling into the PEO with period 4. Next, we define stabilities of a TBPO.

**Definition 3.** A TPEO (TBPO) is said to be *locally stable* if at least one EPP falls into the TPEO. A TPEO is said to be *globally stable* if all the EPPs fall into the TPEO. A TPEO is said to be *uniformly stable* if the TPEO is globally stable and the almost same number of EPPs fall into each TPEP.

In Fig. 3, the red orbit is the TPEO with period 4 consisting of the first to the fourth TPEPs. In Fig. 3(a), all the EPPs fall into the TPEO hence the TPEO is globally stable. In Fig. 3(b), three EPPs fall into each TPEP hence the TBPO is uniformly stable. The uniform stability corresponds to proportional retrieval of the TBPO.

Note that, as $p$ increases, the number of EPPs decreases. Especially, if $p=2^N$ then the TBPO is an M-sequence and EPP does not exist. The definition of stability is based on the EPPs and a suitable number of EPPs are necessary. Since it is hard to determine the upper limit of $p$, in this paper, we consider TBPOs which satisfy

$$p\leq N \tag{14}$$

based on engineering applications in Section 5. Note that if the Dmap has only one PEO then the PEO is globally stable, because

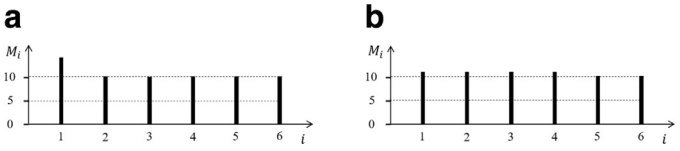


**Fig. 4.** Histograms for $N = 6$ and $p = 6$ $(10 < 2^6/6 < 11)$. (a) $M_{min} = 10$, $M_{max} = 14$, $\beta = 10/11$. (b) $M_{min} = 10$, $M_{max} = 11$, $\beta = 1$.

any point in $L_N$ (the domain of Dmap in Eq. (3)) is either a PEP or an EPP.

In order to characterize stability of a TPEO, we present two simple feature quantities. The first quantity is defined by

$$\alpha = \frac{\text{The number of initial points falling into a TPEO}}{2^N} \tag{15}$$

where $p/2^N \le \alpha \le 1$. A TPEO is globally stable if $\alpha = 1$ and is locally stable if $\alpha > p/2^N$. In order to define the second quantity, we introduce a histogram:

$$M_i = \text{The number of initial points falling into the } i\text{th TPEP} \tag{16}$$

where $i \in \{1, 2, \ldots, p\}$. Since the initial points include the $i$th TPEP, $(M_i - 1)$ is the number of EPPs falling into the $i$th TPEP. Fig. 3(a) shows a histogram for a globally stable TPEO where 8, 1, 2, and 1 EPPs fall into the first, second, third, and fourth TPEPs, respectively: $\{M_1.M_2, M_3, M_4\} = \{9, 2, 3, 2\}$. Fig. 3(b) shows a histogram for a uniformly stable TPEO where 3 EPPs fall into each TPEP: $\{M_1.M_2, M_3, M_4\} = \{4, 4, 4, 4\}$. Let $M_{min}$ denote the minimum value of $M_i$ for $i = 1 \sim p$ and let $M_{max}$ denote the maximum value of $M_i$ for $i = 1 \sim p$. If the period $p$ is a divisor of $2^N$ then the second feature quantity is defined by

$$\beta = \frac{M_{min}}{m}, \quad m = \frac{2^N}{p} \tag{17}$$

where $p/2^N \le \beta \le \alpha \le 1$. The inequality $\beta \le \alpha$ is derived from $M_{min} \le 2^N\alpha/p$ and $\beta = pM_{min}/2^N$. If $M_{min} = 2^N/p$ then $M_i$ must be $2^N/p$ for all $i = 1 \sim p$. Hence a TPEO is uniformly stable if $\beta = 1$. As a TBPO is given, its stability is characterized by $(\alpha, \beta)$. The globally stable TPEO in Fig. 3(a) is characterized by $(\alpha, \beta) = (16/16, 2/4)$. The uniformly stable TPEO in Fig. 3(b) is characterized by $(\alpha, \beta) = (16/16, 4/4)$. In the stabilization method SES defined afterward, the feature quantities $\beta$ and $\alpha$ are used to evaluate stability of a TBPO. The goal of the SES is $(\alpha, \beta) = (1, 1)$.

If the period $p$ is not a divisor of $2^N$, the uniform distribution like Fig. 3(b) is impossible. In this case, the second feature quantity is defined by

$$\beta = \begin{cases} 1 & \text{if } M_{min} = m - 1, \ M_{max} = m \\ \dfrac{M_{min}}{m} & \text{otherwise,} \end{cases} \tag{18}$$

where $m$ is an integer such that $m - 1 < 2^N/p < m$. Fig. 4(a) shows a histogram where $(M_{min}, M_{max}) = (10, 14)$ and $\beta = 10/11$ for $2^N = 64$ and $p = 6$ $(10 < 64/6 < 11)$. Fig. 4(b) shows a histogram where $(M_{min}, M_{max}) = (10, 11)$ and $\beta = 1$. As a formal definition, let $\beta = 0$ if the TPEO (TBPO) is not stored into the DBNN.

It should be noted that, in order to calculate the feature quantities $\beta$ and $\alpha$, we must check $2^N$ points in the domain of the Dmap in Eq. (3). Because of "the curse of dimensionality", the calculation becomes impossible as $N$ increases and some approximation method is necessary. In Sections 5 and 6, we calculate the feature quantities exactly for $N = 6$ based on engineering applications.

In order to define the SES, we introduce several basic notations. Let $s$ denote a generation of evolution and let $S_{max}$ denote the maximum limit of $s$. Let $V^l \equiv (V^l_{11}, \ldots, V^l_{NN})$, $V^l_{ij} \in \{-1, 0, +1\}$, denote the $l$th individuals where $l \in \{1, 2, \ldots, K(s)\}$. The $V^l$ corresponds to the connection parameters $\{w_{ij}\}$ and $K(s)$ is the number of individuals at step $s$. Let $K_{max}$ denote the upper limit of $K(s)$. We define the SES that aims at uniform stabilization of a TPEO (TBPO) stored into the DBNN.

**Step 1** (Initialization): let $s = 0$ and let $K(0) = 1$. The individual $V^1$ is initialized by connection parameters (e.g., Eq. (13)) that guarantees storage of a TPEO. $s \leftarrow s + 1$ and go to Step 2.

**Step 2** (Zero-insertion): replacing one element of each individual $V^l = (V^l_{11}, \ldots, V^l_{NN})$ with zero:

$$\begin{matrix} (0, & V^l_{12}, & V^l_{13}, & \cdots, & V^l_{NN}) \\ (V^l_{11}, & 0, & V^l_{13}, & \cdots, & V^l_{NN}) \\ & & & \ddots & \\ (V^l_{11}, & V^l_{12}, & V^l_{13}, & \cdots, & 0), \end{matrix} \tag{19}$$

we obtain $N \times N \times K(s)$ individuals. If some individual $V^l$ includes a zero element, e.g., $V^l_{12} = 0$, then the individual is not changed by the zero-insertion and is preserved. This preservation can avoid lost of a good individual. One individual corresponds to one set of ternary connection parameters from which the threshold parameters $T_i$ are given by Eqs. (11) or (12).

**Step 3** (Evaluation): the individuals are evaluated by the feature quantity $\beta$. Let $K_\beta$ be the number of individuals that gives the best value of $\beta$ in the past history. If $K_\beta \le K_{max}$, then the $K_\beta$ individuals are preserved. $K(s) \leftarrow K_\beta$ and go to Step 4. If $K_\beta \ge K_{max}$ then the $K_{max}$ individuals are selected randomly and are preserved. $K(s) \leftarrow K_{max}$ and go to Step 4.

**Step 4** (Termination): if $\beta = 1$ then the algorithm is terminated. Note that, referring to the inequality $\beta \le \alpha \le 1$ of Eq. (17), $\beta = 1$ guarantees $\alpha = 1$.

**Step 5** (Termination): let $s \leftarrow s + 1$, go to Step 2, and repeat until the maximum step limit $S_{max}$.

We refer to this algorithm as SES1 because it uses 1 feature quantity $\beta$ in Step 3. Replacing the Step 3 with the following Step 3', we define another algorithm.

**Step 3'** (Evaluation): the individuals are evaluated by $\beta$. Let $K_\beta$ be the number of individuals that gives the best value of $\beta$ in the past history. If $K_\beta \ge K_{max}$ then the $K_{max}$ individuals are selected randomly and are preserved. $K(s) \leftarrow K_{max}$ and go to Step 4. If $K_\beta < K_{max}$ then the other individuals are evaluated by $\alpha$. Let $K_\alpha$ be the number of individuals that gives the best value of $\alpha$ in the past history. If $K_\alpha + K_\beta \le K_{max}$ then the $(K_\alpha + K_\beta)$ individuals are preserved. $K(s) \leftarrow (K_\alpha + K_\beta)$ and go to Step 4. If $K_\alpha + K_\beta > K_{max}$, then the $K_{max}$ individuals are selected randomly and are preserved. $K(s) \leftarrow K_{max}$, and go to Step 4.

We refer to this algorithm as SES2 because it uses 2 feature quantities $\beta$ and $\alpha$. In Step 3 of SES1, the individuals are evaluated by only $\beta$, however, the SES1 sometimes fails to increase $\beta$ by a trap of a local optimum. In Step 3' of the SES2, individuals are evaluated by primary feature quantity $\beta$ and secondary feature quantity $\alpha$. The second evaluation by $\alpha$ is able to make better individuals than SES1 as shown in Section 5.

In the SES, the zero-insertion in Step 2 is a key point. The zero-insertion corresponds to wire cutting in a hardware and can reduce power consumption. In order to search a set of the zero elements in $N^2$ connection parameters, the number of evaluations is at most $K_{max} \times N^2 \times S_{max}$ in the SES. Although the most primitive method is the brute force search of an optimal set of zero elements that realizes the strongest uniform stability,[3] the computation efficiency is very bad. The SES is simpler and faster than existing algorithms which utilize the genetic algorithm (GA) [1,2]. The GA is based on stochastic operators such as the elite strategy, muta-

[3] The search space is $(2^{N^2})$ and that of the ternary connections is $(3^{N^2})$.

**Table 1**
TPEO1 from a simple AC/DC converter.

| | | | | | | |
|---|---|---|---|---|---|---|
| $z^1$ | +1 | −1 | −1 | −1 | −1 | +1 |
| $z^2$ | +1 | +1 | −1 | −1 | −1 | −1 |
| $z^3$ | −1 | +1 | +1 | −1 | −1 | −1 |
| $z^4$ | −1 | −1 | +1 | +1 | −1 | −1 |
| $z^5$ | −1 | −1 | −1 | +1 | +1 | −1 |
| $z^6$ | −1 | −1 | −1 | −1 | +1 | +1 |

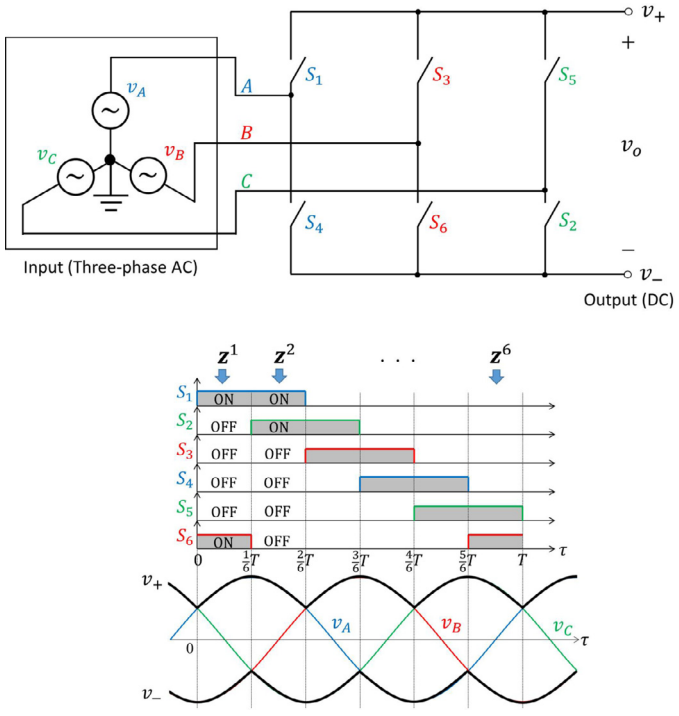


**Fig. 5.** TBPO1 from control signal of a simple AC/DC converter.

tion, and crossover with random selection. The SES does not use the stochastic operators but a simple selection method in Step 3'.

The zero-insertion can reinforce the uniform stability in numerical experiments in Section 6. Although it is very hard to give a theoretical evidence for the reinforcement of stability, we try a rough explanation.

Since $w_{ij}x_j = w_{ij}(-x_j) = 0$ for $w_{ij} = 0$, the zero insertion can help to make plural to one mapping for a new EPP. We show a simple example. Let $\boldsymbol{x} = (x_1, \ldots, x_j, \ldots, x_N)$ correspond to an EPP and let $\boldsymbol{y} = (y_1, \ldots, y_N)$ denote its image:

$$y_i = F(X_i),\ X_i \equiv w_{i1}x_1 + \cdots + w_{ij}x_j + \cdots + w_{iN}x_N - T_i \tag{20}$$

where $i = 1 \sim N$. Inverting the $j$th element $x_j$, we obtain $\boldsymbol{x}' = (x_1, \ldots, -x_j, \ldots, x_N)$. Let $\boldsymbol{x}$ not correspond to an EPP and let $\boldsymbol{y}' = (y'_1, \ldots, y'_N)$ denote its image:

$$y'_i = F(X'_i),\ X'_i \equiv w_{i1}x_1 + \cdots - w_{ij}x_j + \cdots + w_{iN}x_N - T_i \tag{21}$$

Let $w_{ij}x_j = +1$, $y_k = +1$, $y'_k = -1$, and let $y_i = y'_i$ for $i \neq k$. In this case, $X_k = 1$ and $X'_k = -1$ are satisfied. Inserting 0 into $w_{ij}$, we obtain $X_k = X'_k = 0$ hence $y_k = y'_k = +1$. That is, the zero-insertion makes a new EPP $\boldsymbol{y}'$.

## 5. Examples from switching circuits

In this section, we apply the SES to uniform stabilization of two examples. The first example is a 6-dimensional TPEO with period 6 (TPEO1) in Table 1. The TPEO1 is applicable to control a simple AC/DC converter as shown in Fig. 5. In the figure, the 3-phase AC input ($v_A$, $v_B$, $v_C$) with period $T$ is converted into a DC-like output

**Table 2**
Parameters of DBNN for TPEO1 after the CL-based learning.

| $i$ | $w_{i1}$ | $w_{i2}$ | $w_{i3}$ | $w_{i4}$ | $w_{i5}$ | $w_{i6}$ | $T_i$ |
|---|---|---|---|---|---|---|---|
| 1 | +1 | −1 | −1 | −1 | +1 | +1 | +2 |
| 2 | +1 | +1 | −1 | −1 | −1 | +1 | +2 |
| 3 | +1 | +1 | +1 | −1 | −1 | −1 | +2 |
| 4 | −1 | +1 | +1 | +1 | −1 | −1 | +2 |
| 5 | −1 | −1 | +1 | +1 | +1 | −1 | +2 |
| 6 | −1 | −1 | −1 | +1 | +1 | +1 | +2 |

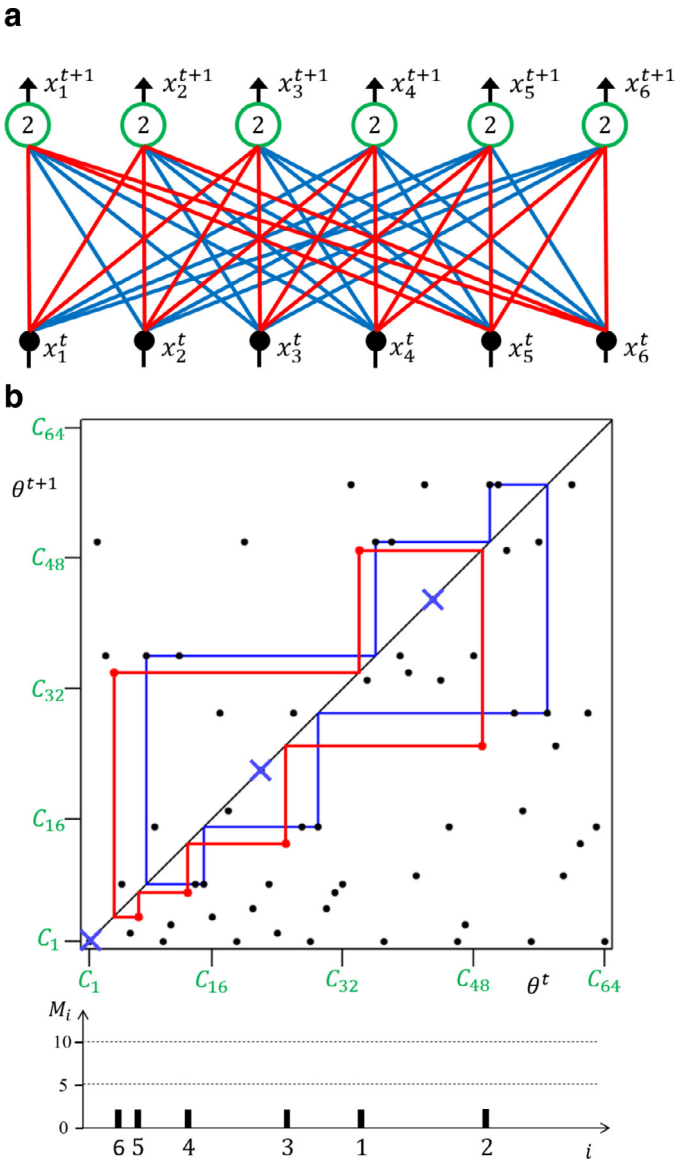


**Fig. 6.** DBNN for TPEO1 after the CL-based learning. (a) Network configuration. (b) Dmap with TPEO1 (red (light gray) orbit) and a spurious PEO (blue (gray) orbit). Histogram of initial points falling into the TPEO1. $\alpha = 12/64$, $\beta = 2/11$.

$v_o$ via 6 switches $S_1$ to $S_6$. The 6 switches are controlled by the TPEO1: $S_i$ =on if $z_i^\tau = +1$ and $S_i$ =off if $z_i^\tau = -1$ for $i = 1 \sim 6$. One step of the TPEO1 corresponds to 1/6 period ($T$/6) of the AC input. Applying the CL-based learning, the TPEO1 can be stored into the DBNN. Table 2 shows parameters after the CL-based learning. Fig. 6 shows DBNN and Dmap where $\alpha = 12/64$ and $\beta = 2/11$.

In order to increase $\beta$, we apply the SES1 to the TPEO1. If $\beta$ increases then uniform stability of the TPEO1 is considered to be reinforced. The value $\beta = 1$ is the goal of the uniform stabilization

**Table 3**
Parameters of the best individual of SES1 for TPEO1 at $s = 9$.

| $i$ | $w_{i1}$ | $w_{i2}$ | $w_{i3}$ | $w_{i4}$ | $w_{i5}$ | $w_{i6}$ | $T_i$ |
|---|---|---|---|---|---|---|---|
| 1 | +1 | 0 | 0 | 0 | +1 | +1 | 0 |
| 2 | +1 | 0 | 0 | −1 | −1 | +1 | +1 |
| 3 | +1 | +1 | 0 | −1 | −1 | −1 | +2 |
| 4 | −1 | +1 | +1 | 0 | −1 | −1 | +2 |
| 5 | −1 | −1 | +1 | +1 | +1 | −1 | +2 |
| 6 | −1 | −1 | −1 | 0 | +1 | 0 | +2 |

**Table 4**
TPEO2 from a simple DC/AC converter.

| | | | | | | |
|---|---|---|---|---|---|---|
| $\boldsymbol{z}^1$ | +1 | −1 | −1 | −1 | +1 | +1 |
| $\boldsymbol{z}^2$ | +1 | +1 | −1 | −1 | −1 | +1 |
| $\boldsymbol{z}^3$ | +1 | +1 | +1 | −1 | −1 | −1 |
| $\boldsymbol{z}^4$ | −1 | +1 | +1 | +1 | −1 | −1 |
| $\boldsymbol{z}^5$ | −1 | −1 | +1 | +1 | +1 | −1 |
| $\boldsymbol{z}^6$ | −1 | −1 | −1 | +1 | +1 | +1 |

**Table 5**
Parameters of DBNN for TPEO2 after the CL-based learning.

| $i$ | $w_{i1}$ | $w_{i2}$ | $w_{i3}$ | $w_{i4}$ | $w_{i5}$ | $w_{i6}$ | $T_i$ |
|---|---|---|---|---|---|---|---|
| 1 | +1 | −1 | −1 | −1 | +1 | +1 | 0 |
| 2 | +1 | +1 | −1 | −1 | −1 | +1 | 0 |
| 3 | +1 | +1 | +1 | −1 | −1 | −1 | 0 |
| 4 | −1 | +1 | +1 | +1 | −1 | −1 | 0 |
| 5 | −1 | −1 | +1 | +1 | +1 | −1 | 0 |
| 6 | −1 | −1 | −1 | +1 | +1 | +1 | 0 |

where $\beta = 1$ guarantees $\alpha = 1$ as stated in Step 4 of the SES. The connection parameters after the CL-based learning ($w_{ij}$ in Table 2) are used as an initial individual. It means that the SES1 must give larger or equal value of $\beta$ than the CL-based learning. The algorithm parameters are selected as the following:

$$K_{max} = 10,\ S_{max} = 20 \tag{22}$$

The $S_{max} = 20$ means that about half elements of connection parameters can be zero. The $K_{max} = 10$ is selected after trial and error. The SES1 can increase $\beta$ and the best individual achieves $\beta = 9/11$ ($\alpha = 64/64$) at $s = 9$. Table 3 shows parameters of the best individual at $s = 9$. Fig. 7 shows the DBNN and Dmap. Fig. 8(a) shows an evolution process of the best individual. Fig. 8(b) shows the number of individuals which varies for $s$. We can see that the zero-insertion is effective to reinforce uniform stability of TPEO1. We have confirmed that the SES2 can realize the almost same result as the SES1.

The second example TPEO2 is shown in Table 4. The TPEO2 is applicable to control a simple DC/AC converter as shown in Fig. 9. The DC inputs $\pm V_s/2$ are converted into 3-phase AC-like output ($v_A$, $v_B$, $v_C$) via 6 switches $S_1$ to $S_6$. Relation between the TPEO2 and 6 switches are the same as the TPEO1. Applying the CL-based learning, the TPEO2 can be stored into the DBNN. Table 5 shows parameters after the CL-based learning. Fig. 10 shows the DBNN and Dmap where $\alpha = 42/64$ and $\beta = 7/11$. Using connection parameters after the CL-based learning (Table 5) as an initial individual, we have applied the SES1, however, $\beta$ cannot be increased from 7/11. The individuals seem to be trapped into some local solution.

We then apply the SES2 with the same initial individual as the SES1. The SES2 can increase $\beta$ and the best individual achieves $\beta = 10/11$ and $\alpha = 1$ at $s = 12$. Table 6 shows parameters of the best individual at $s = 12$.

Fig. 11 shows DBNN and Dmap for the best individual. Fig. 12(a) shows an evolution process of the best individual. Fig. 12(b) shows the number of preserved individuals evaluated by $\beta$ and $\alpha$ for $s$. Fig. 12(c) shows the orbit of the best individual on $\beta - \alpha$ plane in

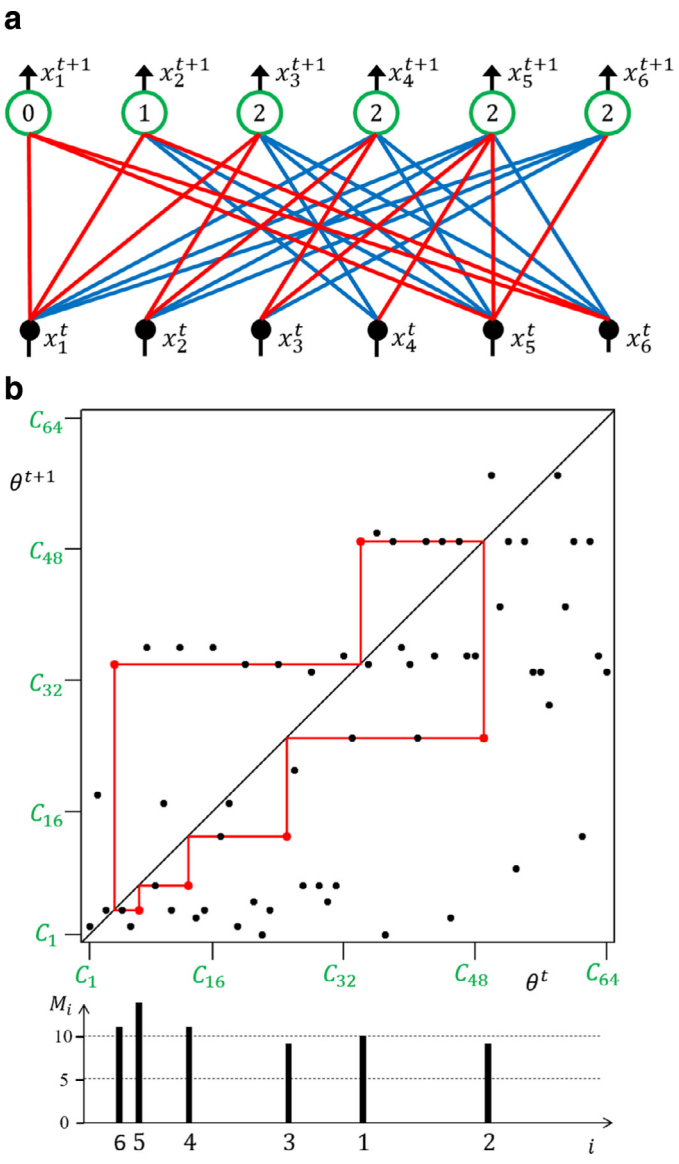


**Fig. 7.** DBNN of the best individual of SES1 for TPEO1. (a) Network configuration. (b) Dmap and histogram of initial points falling into the TPEO1 ($\alpha = 64/64$, $\beta = 9/11$).

**Table 6**
Parameters of the best individual of SES2 for TPEO2 at $s = 12$.

| $i$ | $w_{i1}$ | $w_{i2}$ | $w_{i3}$ | $w_{i4}$ | $w_{i5}$ | $w_{i6}$ | $T_i$ |
|---|---|---|---|---|---|---|---|
| 1 | +1 | −1 | −1 | −1 | +1 | 0 | 0 |
| 2 | 0 | +1 | −1 | −1 | −1 | +1 | 0 |
| 3 | +1 | +1 | 0 | −1 | −1 | −1 | 0 |
| 4 | −1 | 0 | +1 | 0 | 0 | −1 | 0 |
| 5 | −1 | −1 | +1 | +1 | +1 | 0 | 0 |
| 6 | −1 | −1 | −1 | +1 | 0 | +1 | 0 |

the evolution process. We can see that $K_\beta = 0$ and $K_\alpha \geq K_{max}$ at $s = 0$: inserting one zero element into the initial individual, the SES2 cannot increase $\beta$ and can increase $\alpha$. Inserting one zero element into each of the preserved individuals, the SES2 can increase $\beta$ at $s = 2$. We can also see that $K_\beta = 1$ and $K_\beta + K_\alpha \geq K_{max}$ at $s = 10$: the evaluation by $\alpha$ causes decrease of $\beta$ of some individual that can realize $(\beta, \alpha) = (10/11, 1)$ at $s = 12$. In such a case, decrease of $\beta$ seems to be effective to escape from a trap and to generate some individual that is able to approach the goal $(\alpha, \beta) = (1, 1)$.

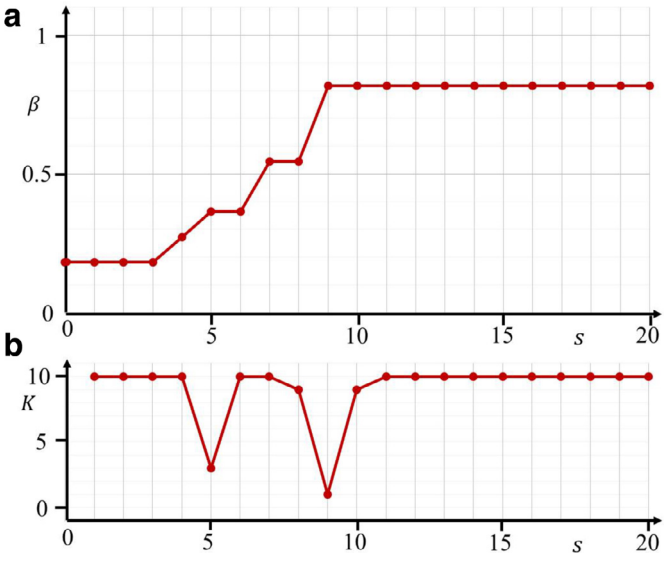


**Fig. 8.** Evolution process of SES1 for TPEO1. (a) $\beta$ of the best individual that reaches 9/11 at $s = 9$. (b) The number of preserved individuals.

It should be noted that one DBNN can be used as control signal generator for plural circuits (e.g., TPEO1 and TPEO2 for AC/DC and DC/AC converters). If the stability can be reinforced then the control becomes robust and reliable. That is, the DBNN is applicable potentially to a robust and reliable reconfigurable control signal generator for switching circuits.

## 6. Numerical experiments and evaluation

In order to investigate stabilization capability of the SES2, we perform numerical experiments for 30 examples of TPEOs such that

$$N = 6,\ \ p = 6,\ \ 2 \le H_d(z^i, z^j) \le 4 \text{ for } |i-j| \ne np \tag{23}$$

where $H_d$ denotes the Hamming distance. The 30 TPEOs include the TPEO1 and TPEO2 in Section 5. The dynamics of $N$-dimensional DBNN is integrated into a Dmap on a set of $2^N$ points. Note again that, as $N$ increases, visualization and analysis become hard (curse of dimensionality). Even in the case $N = 6$, there exist $64^{64}$ Dmaps having various PEOs/EPPs. The number of evaluations is 36!/18! in the brute force of zero-insertion into half of connection parameters.

Applying the CL-based learning, the 30 TPEOs can be stored into the DBNN. The parameters after the CL-based learning are used as initial individuals of the SES2. The results for $(K_{max}, S_{max}) = (10, 20)$ are summarized in Fig. 13 where $\beta_{CL}$ is the value of $\beta$ after the CL-based learning and $\beta_{SES2}$ is the value of $\beta$ of the best individual in the SES2. We can see that almost all the values of $\beta_{CL}$ are far from the optimal value $\beta = 1$. For example, $\beta_{CL} = 1/11$ for 18 TPEOs in the figure. The SES2 can increase the $\beta$ for all the TPEOs where $\alpha = 1$ is confirmed. As a typical example, we have one plot $(\beta_{CL}, \beta_{SES2}) = (1/11, 1)$: the $\beta$ is increased from 1/11 to 1.

In order to investigate influence of $K_{max}$, we have applied SES2 for the same 30 TPEOs as the above for $K_{max} \in \{6, 8, 10, 12, 14\}$ and $S_{max} = 20$. The results are summarized in Table 7 with three measures:

$\beta_{SES2}$ in the minimum, average, and maximum values.
SR: success rate such that $\beta_{SES2} \ge 9/11$ is achieved.
#ITE: the average number of iterations in successful runs.

The value of #ITE$\times$ $K_{max}$ is also shown as the total number of evaluations in successful runs. In Table 7, we can see that the SES2 must increase $\beta$ and the zero-insertion is effective to reinforce the uniform stability. The $\beta_{SES2}$ and SR for $K_{max} = 10$ are better than those for $K_{max} \in \{6, 8\}$ and are almost the same as those for $K_{max} \in \{12, 14\}$. On the other hand, #ITE increases as $K_{max}$ increases. The parameter setting of $K_{max} = 10$ is suitable for the 30 TPEOs. As stated in Section 4, the SES is simpler and the computation costs are lower than the GA-based methods in [1,2]. These results are basic information for developments of the SES2 into various engineering applications.

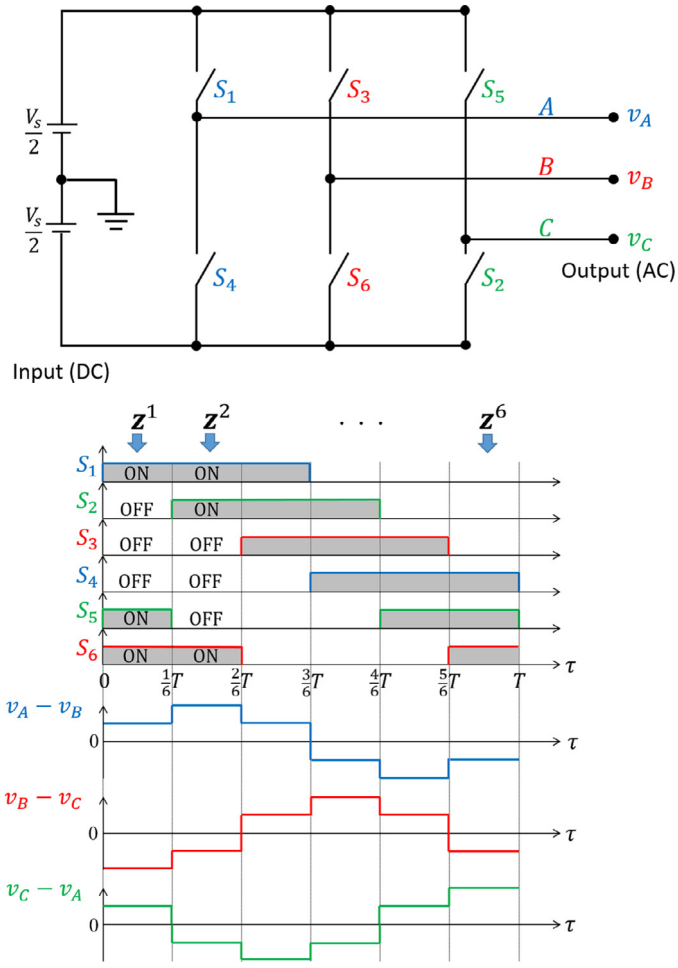


**Fig. 9.** TBPO2 from control signal of a simple DC/AC converter.

**Table 7**
Basic results of SES2 for 30 TPEOs ($\beta_{CL} = 0.17$ in average).

| $K_{max}$ | $\beta_{SES2}$(max/avg/min) | SR(%) | #ITE | #ITE$\times$ $K_{max}$ |
|---|---|---|---|---|
| 6 | 0.91/0.71/0.09 | 40 | 7.2 | 43 |
| 8 | 0.91/0.72/0.27 | 40 | 7.4 | 59 |
| 10 | 1/0.79/0.36 | 63 | 8.8 | 88 |
| 12 | 1/0.79/0.36 | 67 | 9.4 | 112 |
| 14 | 1/0.80/0.36 | 67 | 9.4 | 131 |

## 7. Conclusions

Stabilization of a desired BPO in the DBNN has been studied in this paper. The DBNN has ternary connection parameters and can generate various BPOs. Introducing the Dmap, the DBNN dynamics can be visualized. The global stability and uniform stability of BPOs are defined. The two feature quantities $\alpha$ and $\beta$ are presented to evaluate the global and uniform stabilities, respectively. In order to stabilize the TBPO, the SES2 is presented where the individuals correspond to the ternary connection parameters. In the SES2, one

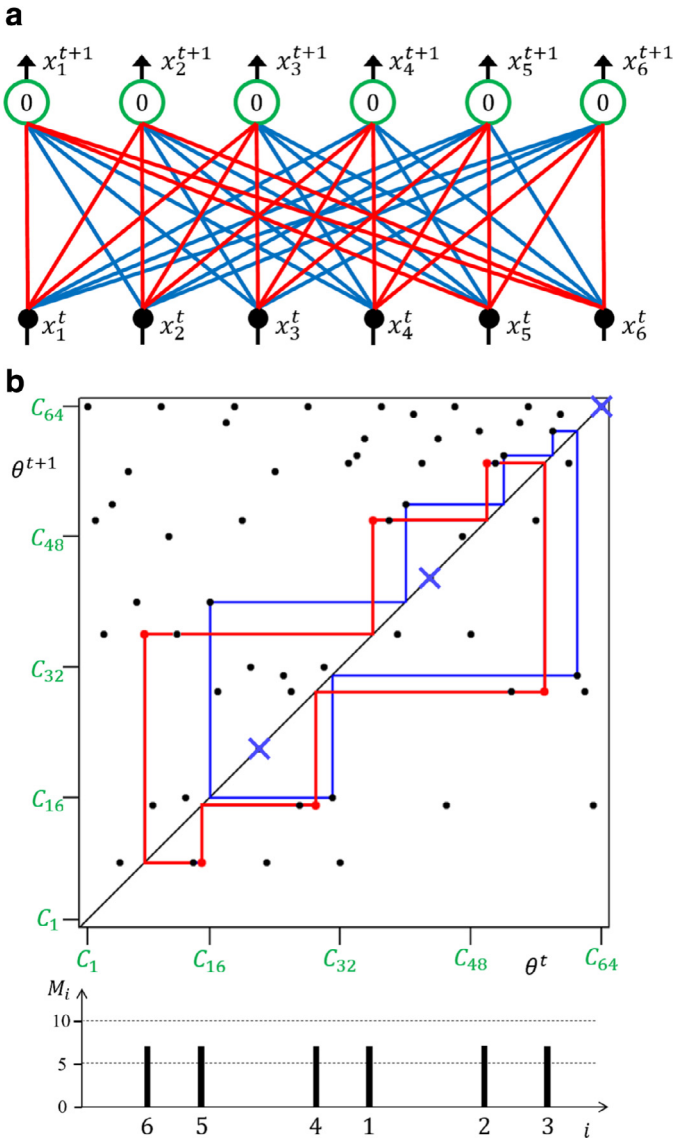


**Fig. 10.** DBNN for TPEO2 after the CL-based learning. (a) Network configuration. (b) Dmap and histogram of initial points falling into the TPEO2 ($\alpha = 42/64$, $\beta = 7/11$).

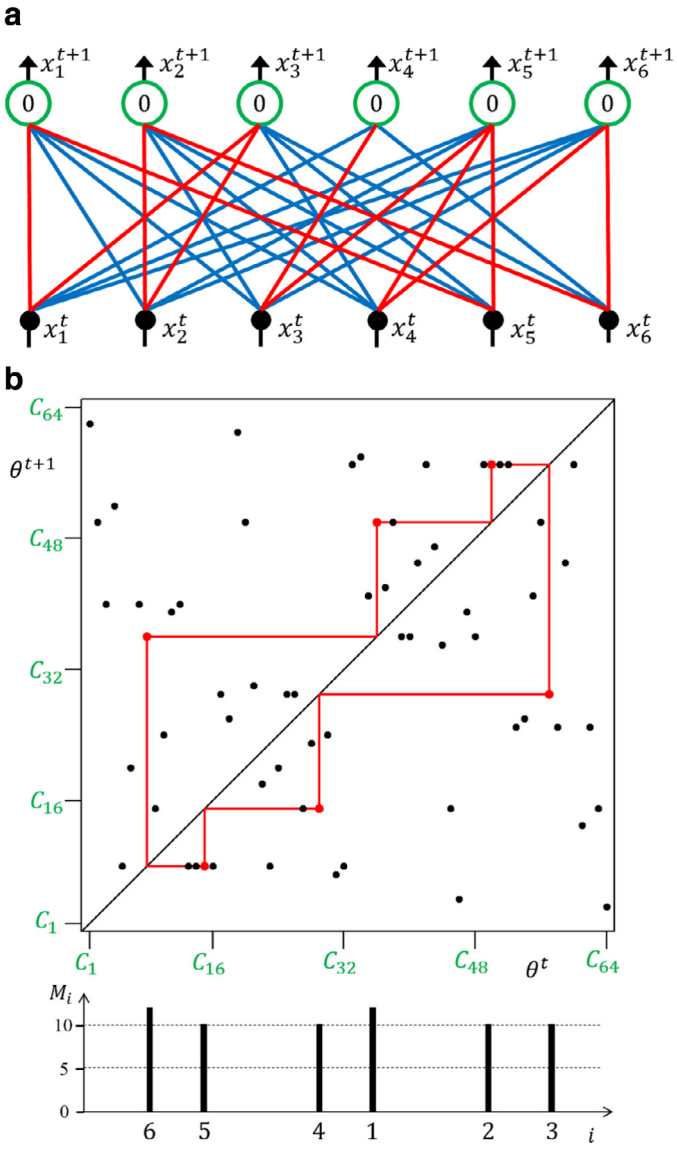


**Fig. 11.** DBNN of the best individual of SES2 for TPEO2. (a) Network configuration. (b) Dmap and histogram of initial points falling into the TPEO2 ($\alpha = 64/64$, $\beta = 10/11$).

zero element is inserted into each individual and the individual is evaluated by the two feature quantities. Performing basic numerical experiments, it has been confirmed that the SES2 can reinforce uniform stability speedily.

Future problems are many, including the following. First, the stabilization process and the effects of the zero-insertion should be considered in more detail. Second, the algorithm parameters (e.g., $K_{max}$) should be optimized for objective TPEOs. Third, for larger $N$, simple feature quantities should be considered for evaluation of stability. As the dimension $N$ increases, calculation of $\beta$ and $\alpha$ becomes impossible. Fourth, the SES2 should be modified for complex global search that is not easy in the SES2 in its present form. Fifth, in order to apply the DBNN and SES to engineering systems, a simple and efficient hardware should be designed by digital circuits. Note that the SES2 is feasible and flexible in application to search of ternary/binary individuals in various engineering systems.

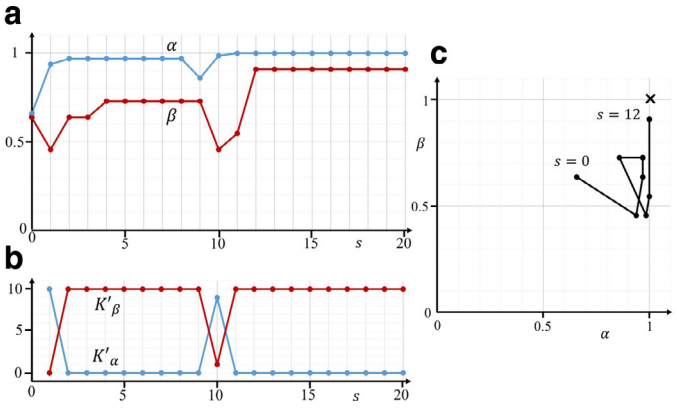


**Fig. 12.** Evolution process of SES2 for TPEO2. (a) Feature quantities $\alpha$ and $\beta$ of the best individual. (b) The number of preserved individuals evaluated by and that by $\alpha$ ($K'_\alpha$). (c) The orbit of the best individual.

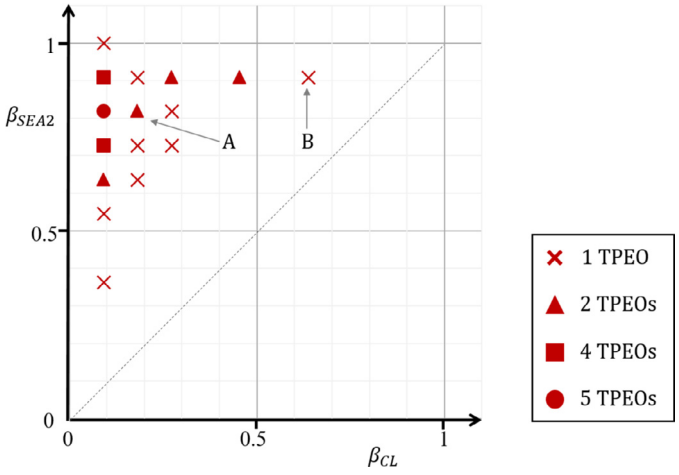


**Fig. 13.** Feature quantity $\beta$ of 30 TPEOs after the CL-based learning ($\beta_{CL}$) and of the best individual in SES2 ($\beta_{SES2}$). In triangle, square, and circle points, plural TPEOs give the same value of ($\beta_{CL}$, $\beta_{SES2}$). $\alpha = 1$ is confirmed for all the points. Point A $(\beta_{CL}, \beta_{SES2}) = (2/11, 9/11)$ and Point B $(\beta_{CL}, \beta_{SES2}) = (7/11, 10/11)$ correspond to TPEO1 and TPEO2, respectively. ($\beta_{SES2} = 0.79$ and $\beta_{CL} = 0.17$ in average).

## Acknowledgment

This work is supported in part by the grants-in-aid for scientific research #15K00350, Japanese Society for the Promotion of Science (JSPS).

## References

[1] R. Kouzuki, T. Saito, Learning of simple dynamic binary neural networks, IEICE Trans. Fundam. E98-D (8) (2013) 1775–1782.
[2] J. Moriyasu, T. Saito, A cascade system of dynamic binary neural networks and learning of periodic orbit, IEICE Trans. Inf. Syst. E98-D (9) (2015) 1622–1629.
[3] R. Sato, T. Saito, Simple feature quantities for learning of dynamic binary neural networks, in: S. Arik, et al. (Eds.), Proceedings of the International Conference on Neural Information Processing, Part I, *Lecture Notes in Computer Science*, vol. 9489, Springer, 2015, pp. 226–233.
[4] D.L. Gray, A.N. Michel, A training algorithm for binary feed forward neural networks, IEEE Trans. Neural Netw. 3 (2) (1992) 176–194.
[5] J.H. Kim, S.K. Park, The geometrical learning of binary neural networks, IEEE Trans. Neural Netw. 6 (1) (1995) 237–247.
[6] F. Chen, G. Chen, Q. He, G. He, X. Xu, Universal perceptron and DNA-like learning algorithm for binary neural networks: non-LSBF implementation, IEEE Trans. Neural Netw. 20 (8) (2009) 1293–1301.
[7] Y. Nakayama, R. Ito, T. Saito, A simple class of binary neural networks and logical synthesis, IEICE Trans. Fundam. E94-A, (9) (2011) 1586–1589.
[8] M. Courbariaux, Y. Bengio, J.-P. David, Binary connect: training deep neural networks with binary weights during propagations, Adv. Neural Inf. Process. Syst. 28 (2015) 3105–3113.
[9] E. Ott, Chaos in Dynamical Systems, Cambridge, 1993.
[10] L.O. Chua, A Nonlinear Dynamics Perspective of Wolfram's New Kind of Science, vol. I, II, World Scientific, 2005.
[11] W. Wada, J. Kuroiwa, S. Nara, Completely reproducible description of digital sound data with cellular automata, Phys. Lett. A 306 (2002) 110–115.
[12] P.L. Rosin, Training cellular automata for image processing, IEEE Trans. Image Process. 15 (7) (2006) 2076–2087.
[13] H. Torikai, A. Funew, T. Saito, Digital spiking neuron and its learning for approximation of various spike-trains, Neural Netw. 21 (2008) 140–149.
[14] T. Iguchi, A. Hirata, H. Torikai, Theoretical and heuristic synthesis of digital spiking neurons for spike-pattern-division multiplexing, IEICE Trans. Fundam. E93-A (8) (2010) 1486–1496.
[15] X. Jiang, V. Gripon, C. Berrou, M. Rabbat, Storing sequences in binary tournament-based neural networks, IEEE Trans. Neural Netw. 27 (5) (2016) 913–925.
[16] L. Szymanski, B. McCane, Deep networks are effective encoders of periodicity, IEEE Trans. Neural Netw. 25 (10) (2014) 1816–1827.
[17] J.J. Hopfield, Neural networks and physical systems with emergent collective computation abilities, Proc. Nat. Acad. Sci. 79 (1982) 2554–2558.
[18] K. Araki, T. Saito, An associative memory including time-variant self-feedback, Neural Netw. 7 (8) (1994) 1267–1271.
[19] J. Vithayathil, Power Electronics, McGraw-Hill, 1992.
[20] B.K. Bose, Neural network applications in power electronics and motor drives – an introduction and perspective, IEEE Trans. Ind. Electron. 54 (1) (2007) 14–33.
[21] J. Rodriguez, M. Rivera, J.W. Kolar, P.W. Wheeler, A review of control and modulation methods for matrix converters, IEEE Trans. Ind. Electron. 59 (1) (2012) 58–70.
[22] S. Amari, A method of statistical neurodynamics, Kybernetik 14 (1974) 201–215.

**Ryuji Sato** received the B.E. degree in electrical and electronics engineering from Hosei University, Tokyo, Japan, in 2015. Now he is working toward the M.E. degree. His research interests are in digital dynamic neural networks and learning algorithms. He is a student member of the IEEE.

**Toshimichi Saito** received the B.E., M. E., and Ph.D. degrees in electrical engineering from Keio university, Yokohama, Japan, in 1980, 1982 and 1985, respectively. He is currently a full professor at Hosei university, Tokyo. His research interests include artificial neural networks, chaos and bifurcation, power electronics, and swarm intelligence. He served in several editorial boards including the IEICE Trans. Fundamentals (1993–1997), the IEEE Trans. Circuits Syst. I (2000–2001), the IEEE Trans. Circuits Syst. II (2003–2005), and the Intl. J. Electronics and Communications (2010–2014). He is a fellow of the IEICE, a senior member of the IEEE, and a member of the JNNS.